Polarisation Measurement and Spin Tracking at the ILC

Moritz Beckmann, Jenny List, Annika Vauth, Benedikt Vormwald

International Workshop on Future Linear Colliders

Tokyo, 14.11.2013

Polarisation for Physics.

Longitudinal polarisation $P_z = \frac{N_R - N_L}{N_R + N_L}$
with $N_{R,L}$: number of right-/left-handed particles in bunch

- SM & BSM: left- and righthanded particles couple differently
  - polarised cross-sections are important observables carrying qualitatively new information!
  - beam polarisation can suppress background / enhance signal
- wanted for physics: luminosity weighted average polarisation at the IP, $\langle P_z \rangle_{IP} = \frac{\int P_z(t)\mathcal{L}(t)dt}{\int \mathcal{L}(t)dt}$
- Note: most physics studies sofar assume this average is known exactly and independently for e^- and e^+ beam.

$P \equiv P_z$ in the following.

Impact of Polarisation Uncertainty.

- SM precision measurements, eg. A_{LR} at Z pole will be limited by polarisation knowledge
  $\longrightarrow$ simultaneous extraction of A_{LR} and $\langle P_{\text{eff}} \rangle_{IP}$

- BSM example: WIMP Dark Matter Search

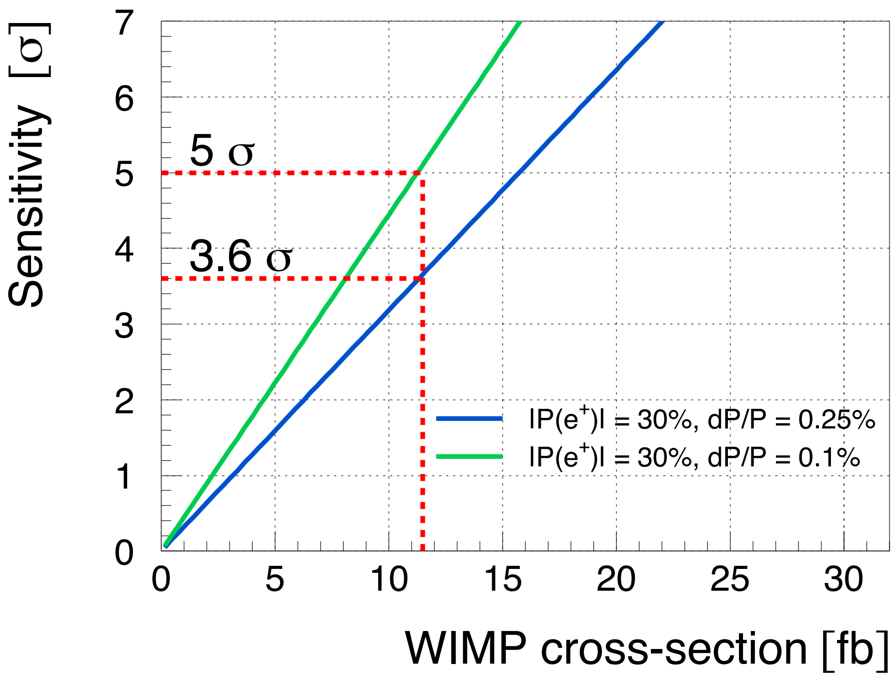

- 500 fb^{-1} at 500 GeV, $|P(e^-, e^+)| = (0.8, 0.3)$
- ILD full simulation incl. systematics
- $dP/P = 0.25\%$
  $\longrightarrow$ "evidence for"
- $dP/P = 0.1\%$
  $\longrightarrow$ "discovery of"

Polarimetry concept for the ILC.

Goal for ILC polarimetry: per mille level precision by combining

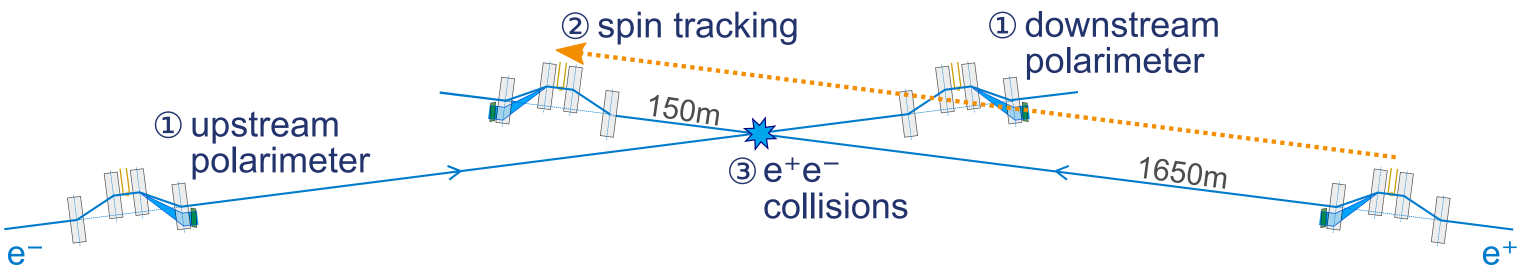

1. Compton polarimeter measurements upstream and downstream of the e^+e^- interaction point
2. Spin tracking studies to relate these measurements to the polarization at the e^+e^- interaction point
3. Long-term average determined from e^+e^- collision data as absolute scale calibration

Compton polarimeters.

- $\mathcal{O}(10^3)$ Compton scatterings/bunch
- Energy spectrum of scattered e^+/e^- depends on polarisation
- Magnetic chicane: energy distibution $\rightarrow$ position distribution
- Measure number of e^+/e^- per detector channel

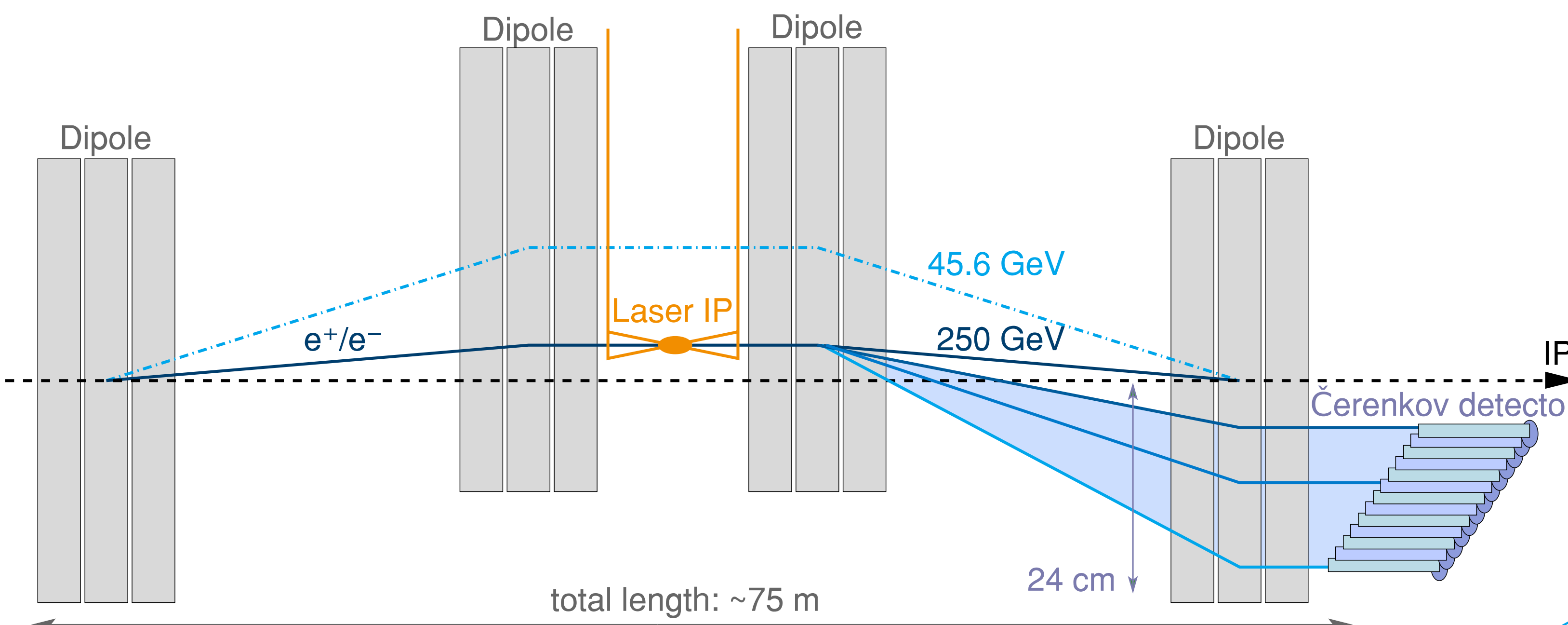

Measurement principle (1).

Compton rate asymmetry is proportional to the beam polarisation:

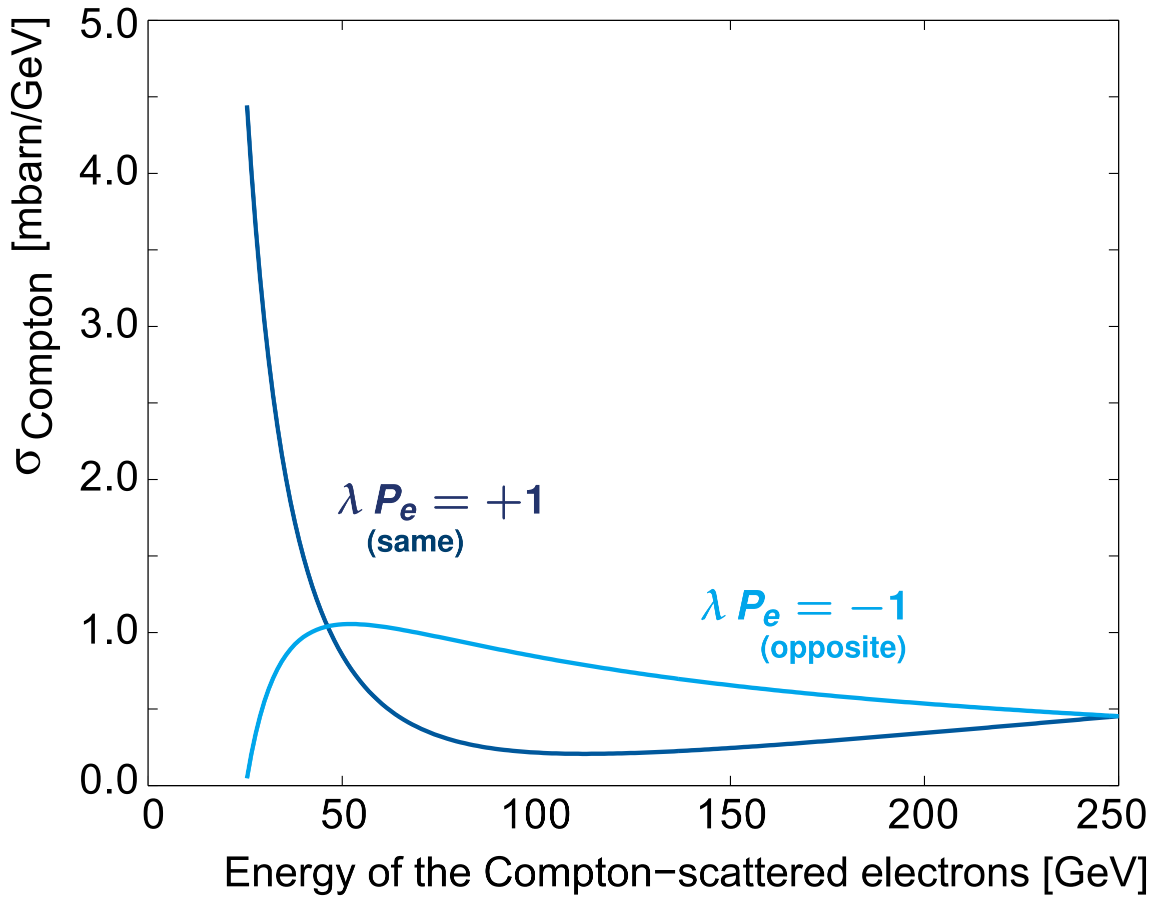

Measurement principle (1).

Compton rate asymmetry is proportional to the beam polarisation:

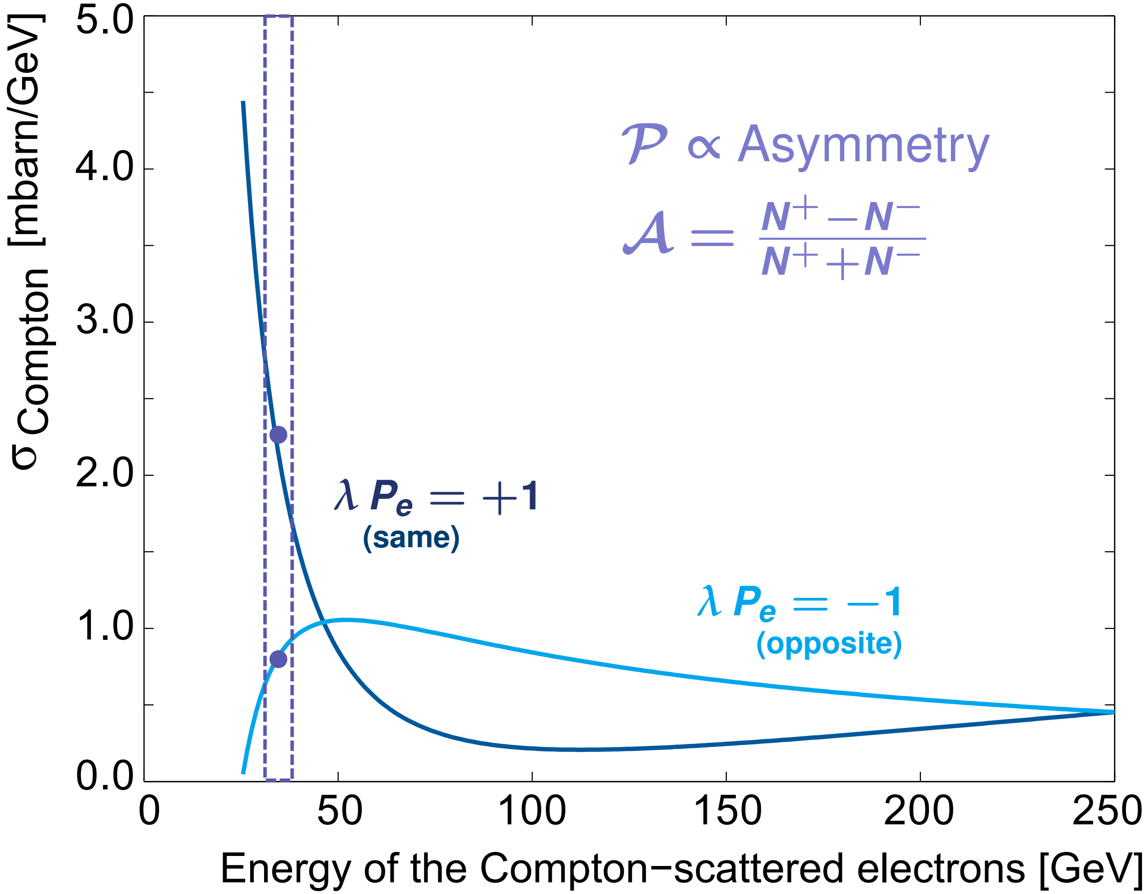

Measurement principle (2).

Magnetic Chicane...

- transforms energy spectrum into spatial distribution
- behind chicane: $\sim$ 20 cm wide
- detect Compton electrons over this area

Detector requirements:

- Total ionising dose up to 100 Mrad / year
- read out signals of 1000-2000 Compton electrons (25-250 GeV) every bunch crossing
- either very linear response or “counting“ electrons
- alignment to $\sim$ 100 µm and $\sim$ 1 mrad
- suppression of background from low energetic particles

Detector Options.

Simple, robust, fast: Cherenkov detectors

- Cherenkov light emission proportional to number of electrons
- independent of electron energy (once relativistic)
- successfully used in best polarimeter sofar at SLC
- gas or quartz option for Cherenkov medium

Detector Options.

Simple, robust, fast: Cherenkov detectors

- Cherenkov light emission proportional to number of electrons
- independent of electron energy (once relativistic)
- successfully used in best polarimeter sofar at SLC
- gas or quartz option for Cherenkov medium

Goal: total uncertainty $\Delta P / P \approx 0.25\,\%$, of which

- laser: $0.1\,\%$
- analysing power (i.e. asymmetry at $\mathcal{P} = 1$): $0.2\,\%$
  $\Rightarrow$ Cherenkov detector design
- detector linearity: $0.1\,\%$ $\Rightarrow$ photodetector calibration

Gas Cherenkov detector.

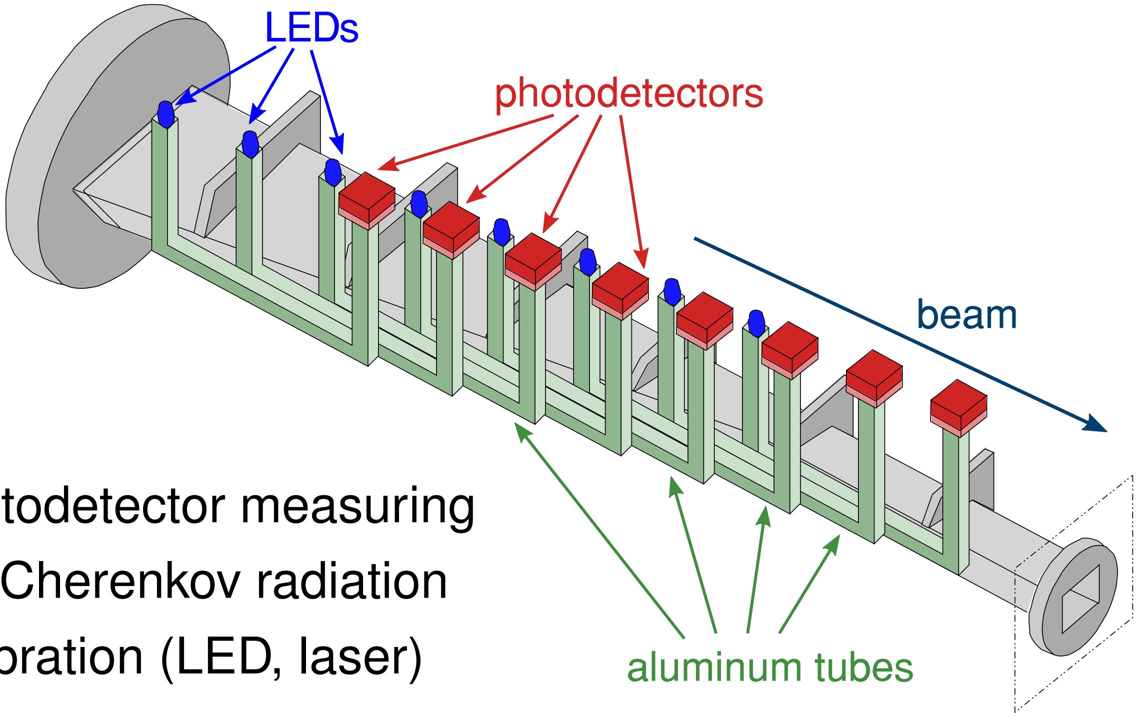

- ➤ **hind U-leg:** photodetector measuring the Cherenkov radiation
- ➤ **front U-leg:** calibration (LED, laser)

Alignment: locate Compton edge in the spectrometer
Segmented photodetectors: Tilt alignments via asymmetries

2-channel prototype tested at ELSA [JINST 7, P01019 (2012)]
$\Rightarrow$ tilt alignment of 0.1°, nearly fulfils alignment requirements

Quartz Cherenkov detector.

Alternative detector concept: quartz detector

- Higher refractive index $\longrightarrow$ higher photon yield
- For enough photons per Compton e^-:
  $\longrightarrow$ calibrate gain directly from the data

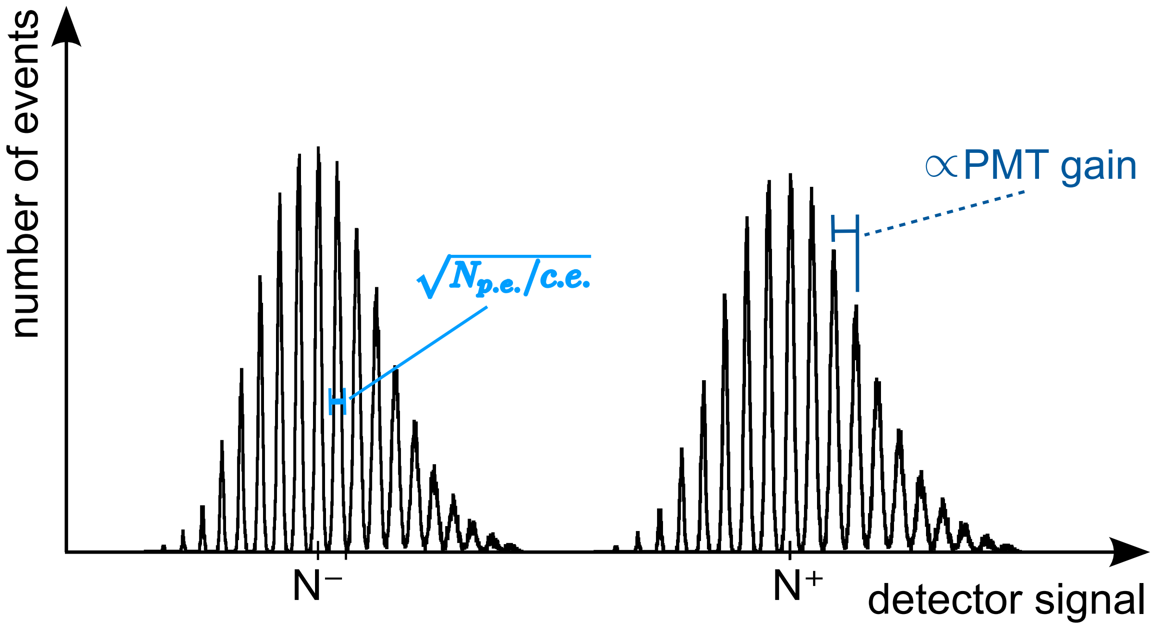

4-channel prototype operated at DESY II testbeam this year.

Calibration of detector non-linearity.

Goal: contribution to overall uncertainty $< 0.1\,\%$

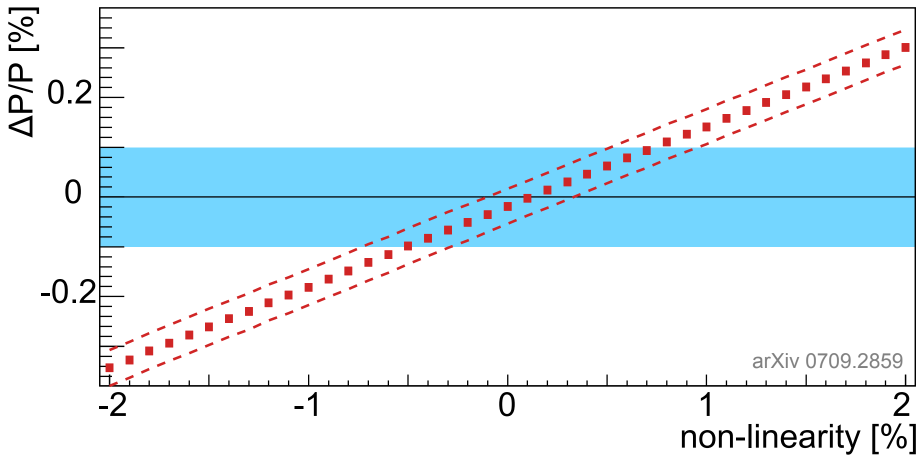

PMTs have to be calibrated to non-linearity $< 0.5\,\%$.

$\mathcal{P} \propto \frac{N^+ - N^-}{N^+ + N^-}$: no absolute calibration needed.

$\longrightarrow$ Differential calibration method using two LEDs:

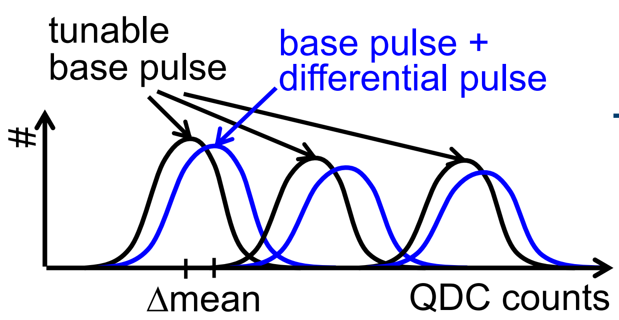

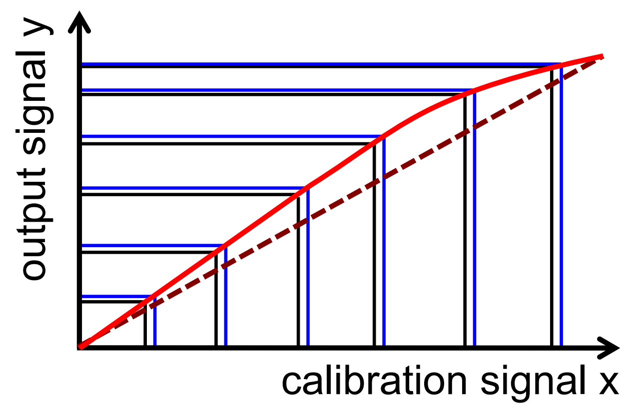

Test of non-linearity correction.

Simulations: Corrections of non-linearities up to 4 % possible.

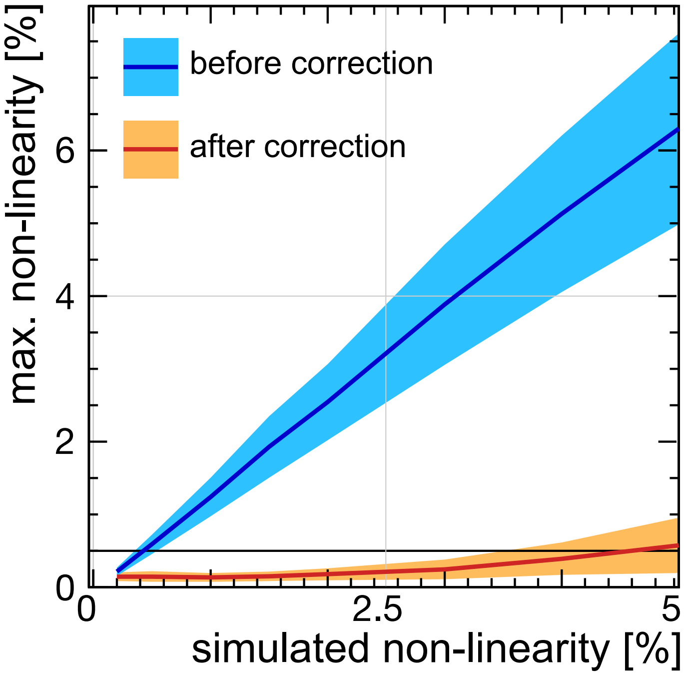

Test of non-linearity correction.

Simulations: Corrections of non-linearities up to 4 % possible.

Applied method to one of the photodetectors used in testbeam:

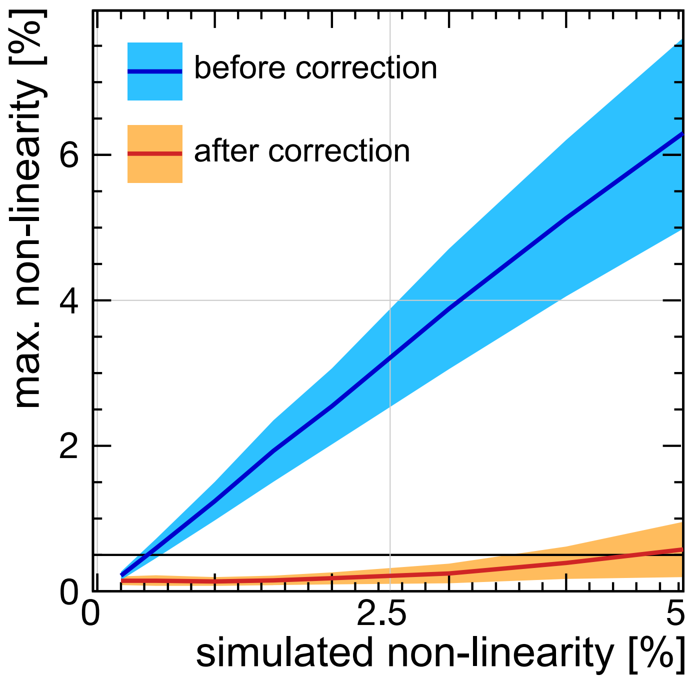

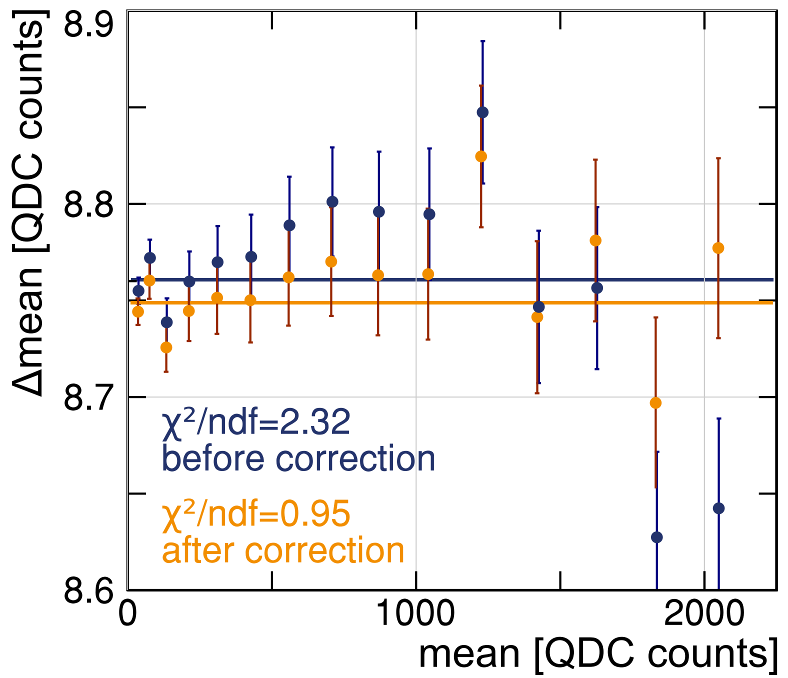

⇒ Reached non-linearity $< 0.2\,\%$ in the expected dynamic range, in single polarimeter channels even smaller.

Introduction

Compton Polarimeters

Compton Polarimetry

Detector R&D

Spin Tracking

Conclusions and Future Plans

Spin Tracking along the BDS.

The Beam Delivery System in the TDR

- upstream polarimeter separated from emittance measurement
- behind the tune-up dump extraction line

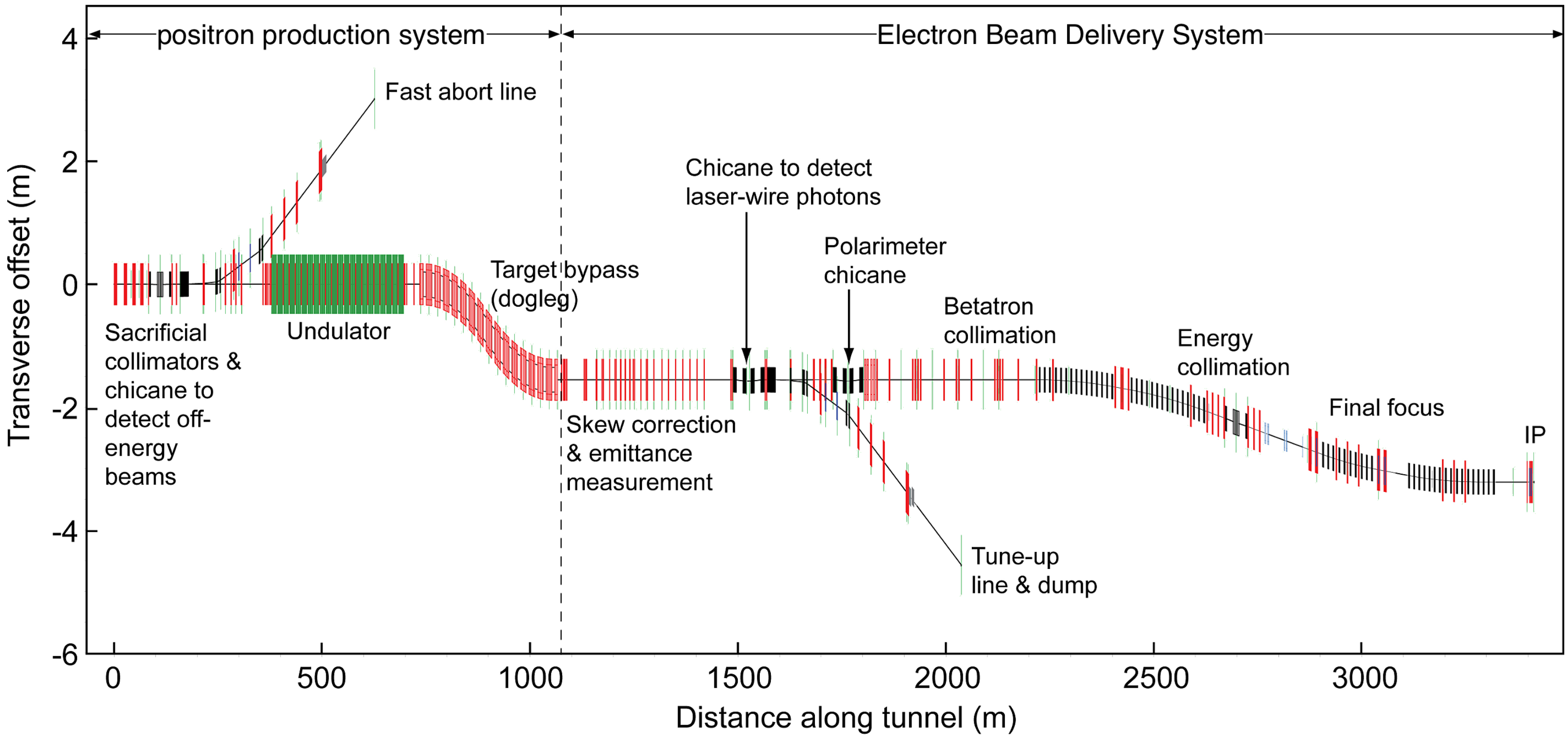

Extraction Line.

Downstream Polarimeter

- located at secondary focus
- 6-magnet chicane kicks Compton $e^{\pm}$ out of synchrotron fan

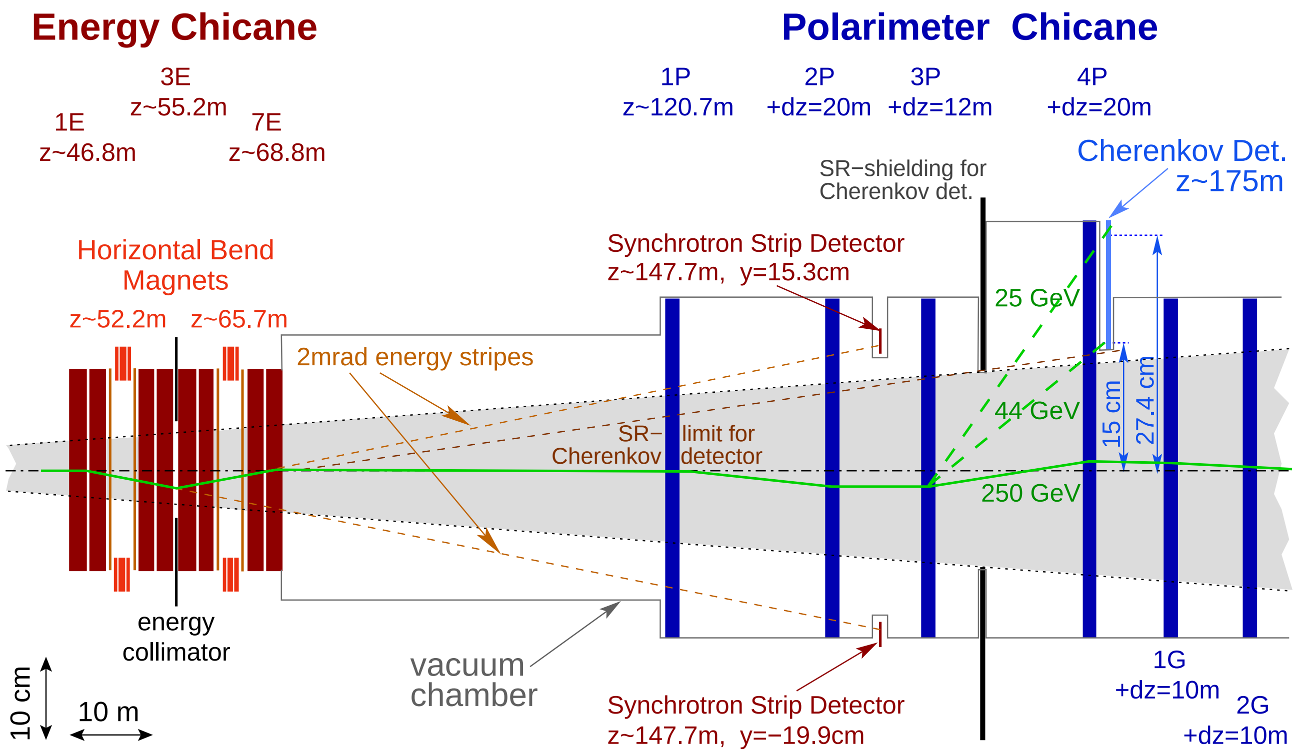

Cross-calibration of Polarimeters.

Without Collisions:
predict value at downstream location from upstream measurement

	effect on $P[10^{-3}]$
Beam and detector alignment at polarimeters ($\Delta\theta_{bunch} = 50\,\mu$rad, $\Delta\theta_{pol} = 25\,\mu$rad)	0.72
Variation in emittances	0.03
Crabbing	< 0.01
Detector magnets	0.01
Emission of synchrotron rad.	0.005
random misalignments (10 µm)	0.43
Total	0.85

Collision Effects.

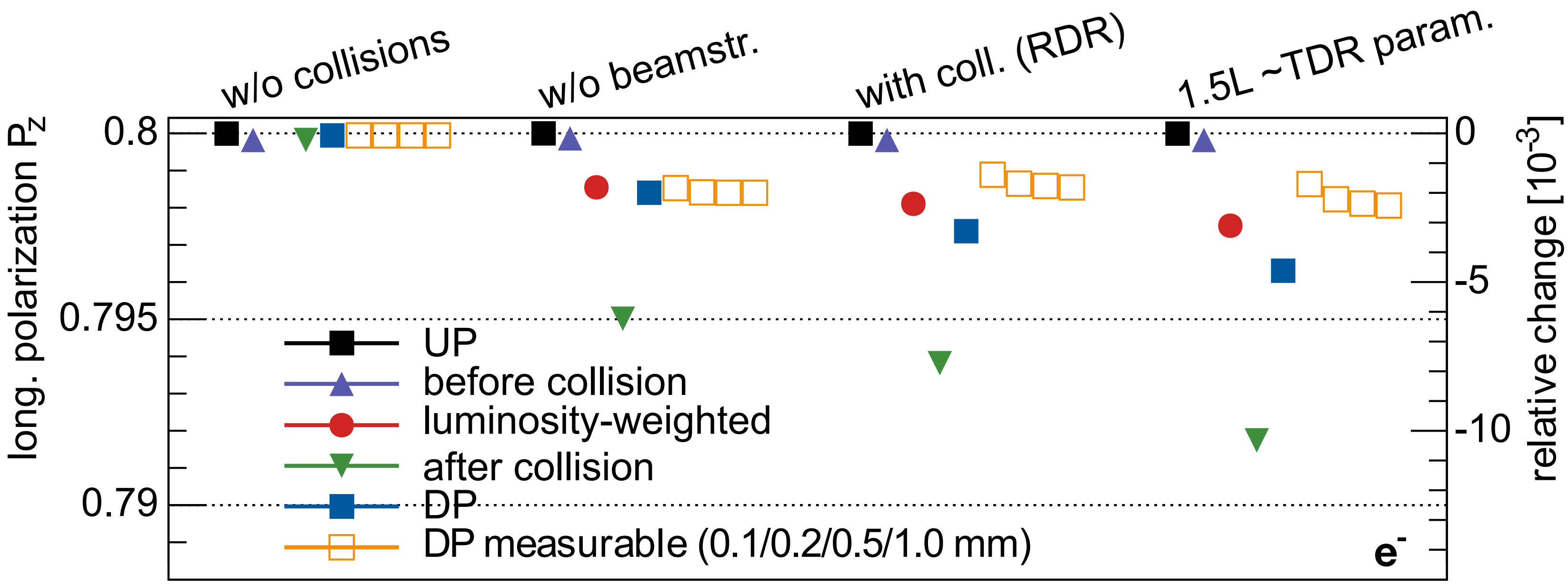

- Without beamstrahlung: extraction line optics retrieves $\langle P \rangle_{IP}$ at downstream polarimeter
- With increasing beamstrahlung (energy loss!): difference to $\langle P \rangle_{IP}$ increases to few permille
- Effect doubles from RDR $\rightarrow$ TDR parameters

Conclusions.

Permille-level precision on lumi-weighted average polarisation at IP required by physics, needs combination of

- scale calibration from e^+e^- collision data
- upstream (UP) and downstream (DP) polarimeters
  - **UP**: time resolution
  - **DP**: collision effects
  - **combined**: cross-check, lumi-weighted polarisation @ IP
- spin tracking and understanding of collision effects

Compton Polarimeters:

- beam-detector alignment & detector linearity crucial
- R&D well underway
- cross-calibration without collisions: $\sim 0.1\%$ from alignment
  - esp. orbit and spin at UP and DP locations (2 km apart)

Next Steps.

Polarisation from collision data:

- systematic evaluation of various approaches → combination?

Luminosity-weighted average polarisation:

- collision effects with TDR beam parameters and lattice
- how to combine polarimeter measurements, luminosity measurement and collision data?

Realisation:

- site specific misalignments, ground motion etc
- revisit laser systems (site specific, new laser technologies...)
- design chicane magnets and vacuum chamber (wide!)
- detectors: prototypes → full-scale, DAQ, ...

Backup Slides .

Compton edge.

Compton edge position nearly independent of beam energy

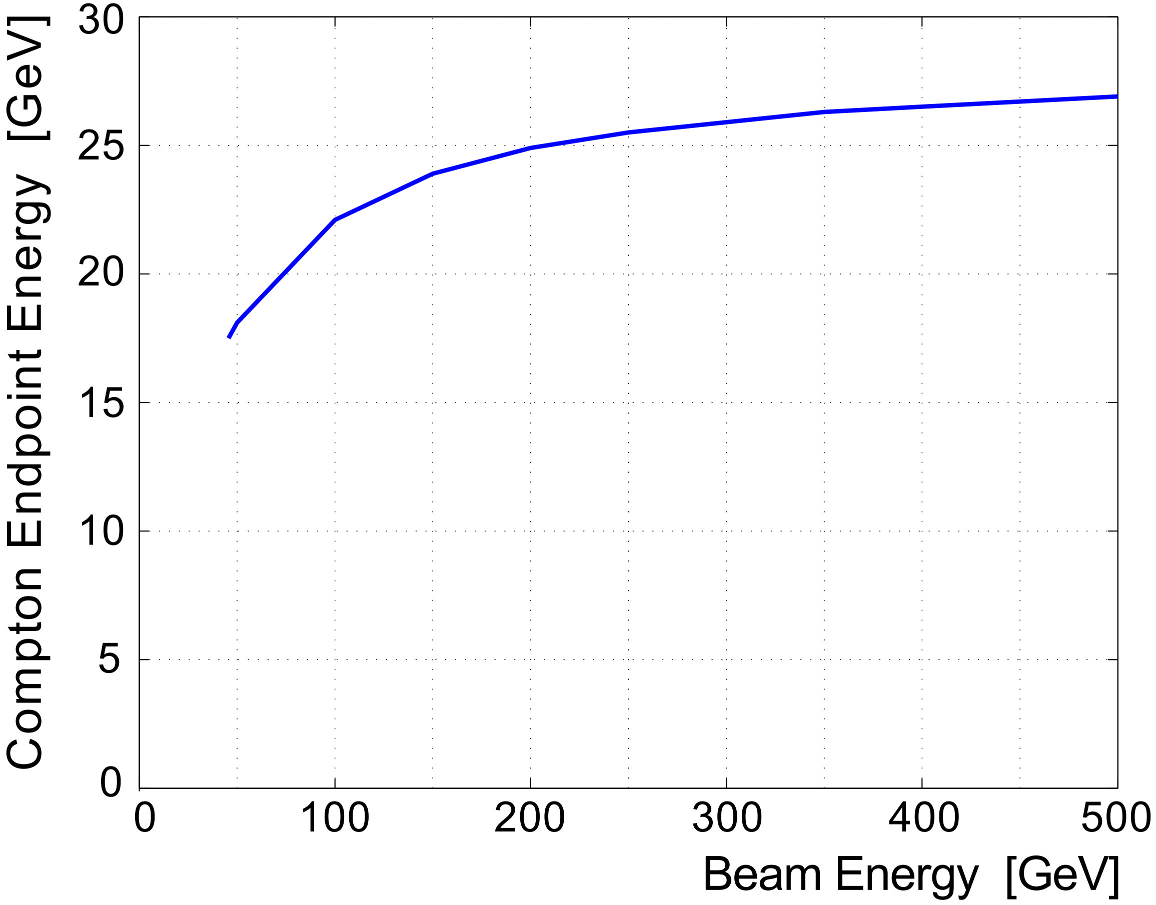

Gas Cherenkov detector: Alignment.

If the detector is tilted

- beam path through the detector varies ⇒ different light path
- different light pattern on the photocathode
  ⇒ alignment via spatial assymetries possible:

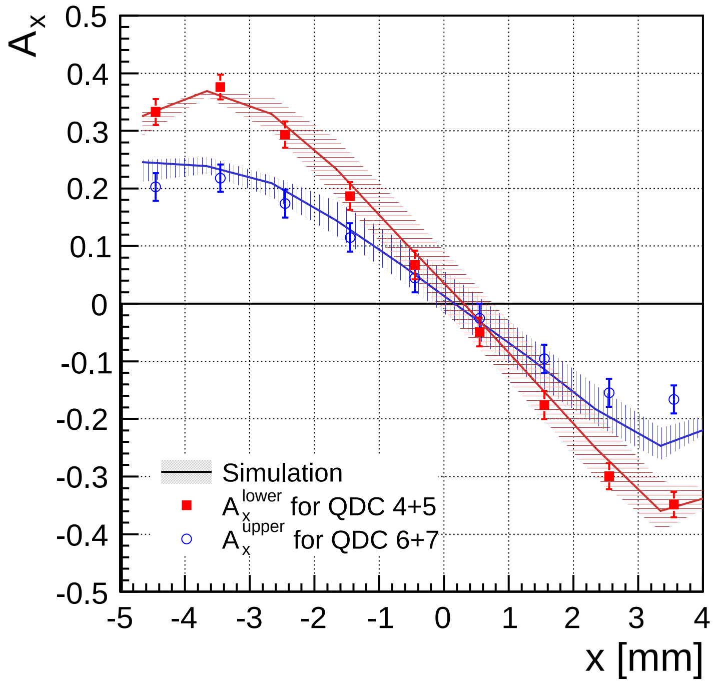

⇒ Reached a tilt alignment of 0.1°. [JINST 7, P01019 (2012)]

Quartz Cherenkov detector prototype.

4-channel prototype operated at DESY II testbeam this year

- channels: quartz bars (5 mm x 18 mm x 100 mm)
- qualitative agreement with simulations (angular dependence, etc.)
- light yield smaller than predicted, studies ongoing

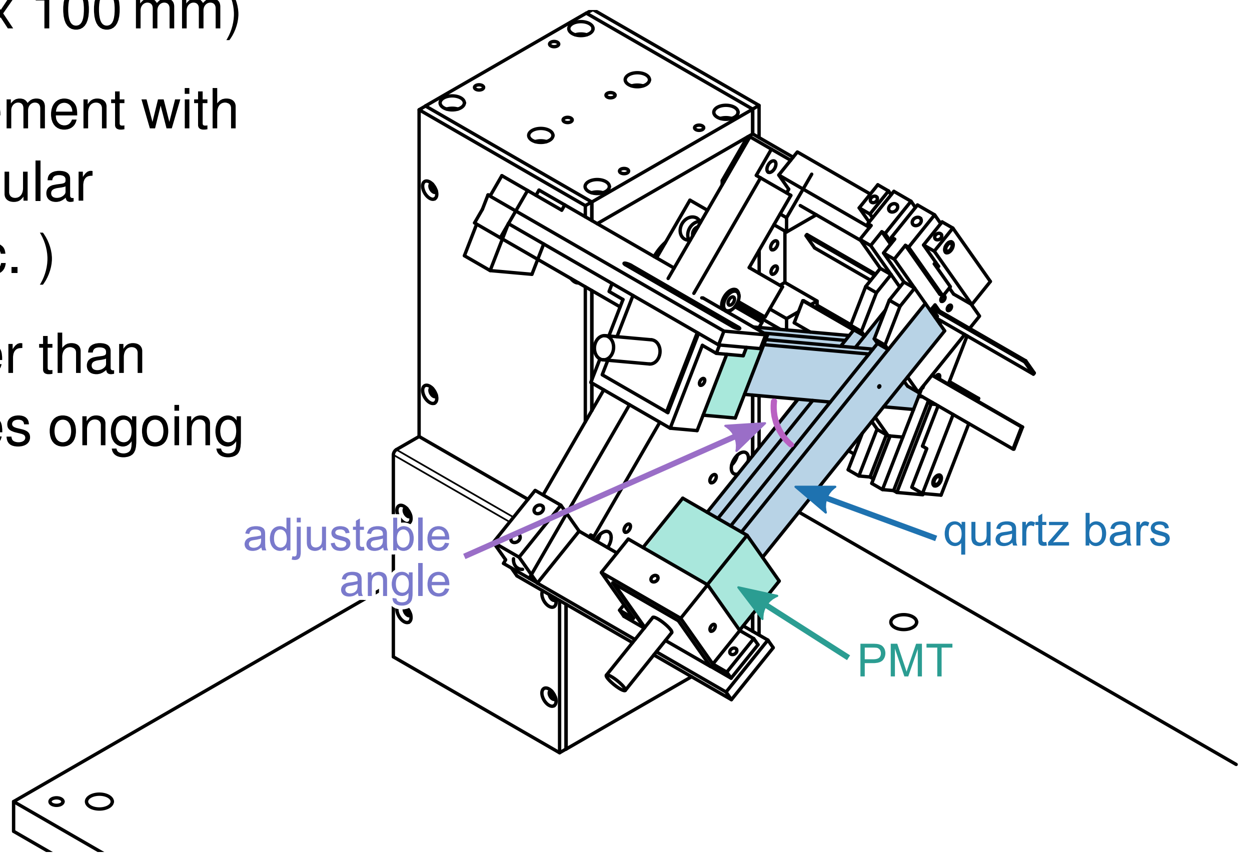

Calibration source requirements.

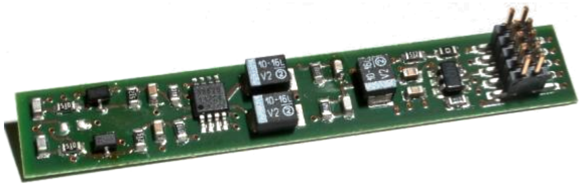

Requirements on the LED driver:

- wave length in UV range ($\lambda = 405\,\text{nm}$)
- applicable in detector design $\longrightarrow$ small
- short light pulses ($< 10\,\text{ns}$)
- coverage of the whole dynamic range of the expected signal
- reproducable and stable light pulses

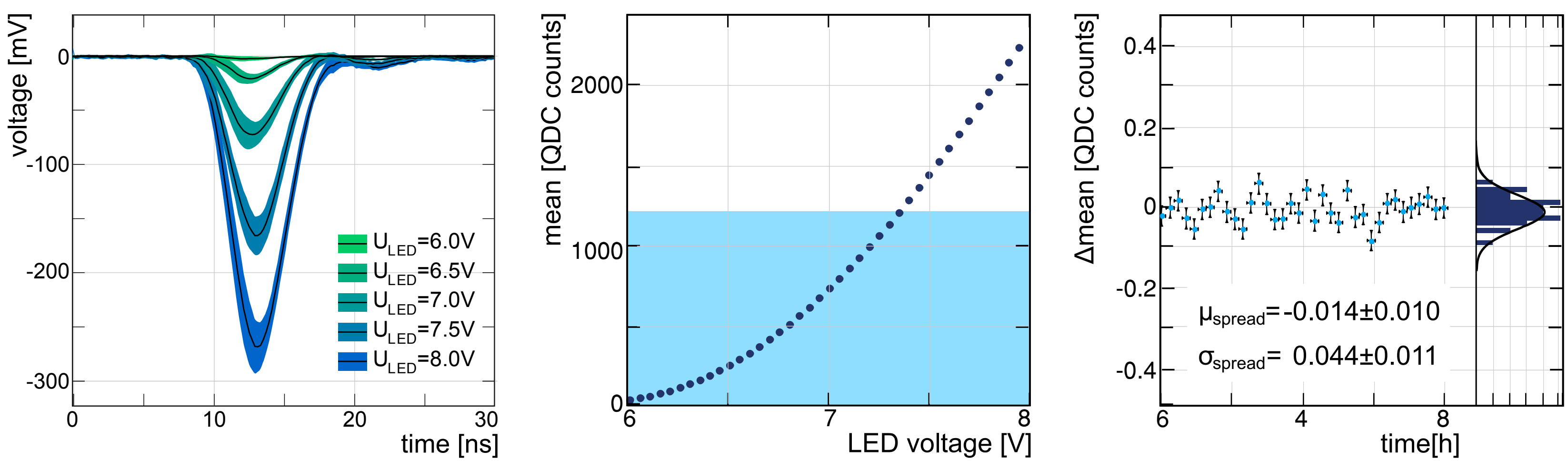

Non-linearity in extreme polarimeter channels.

- up to 210 Compton e^- ($\sim$ 1200 QDC counts)
- overall non-linearity already small in this range (max 0.2 %)
- in single channels even smaller

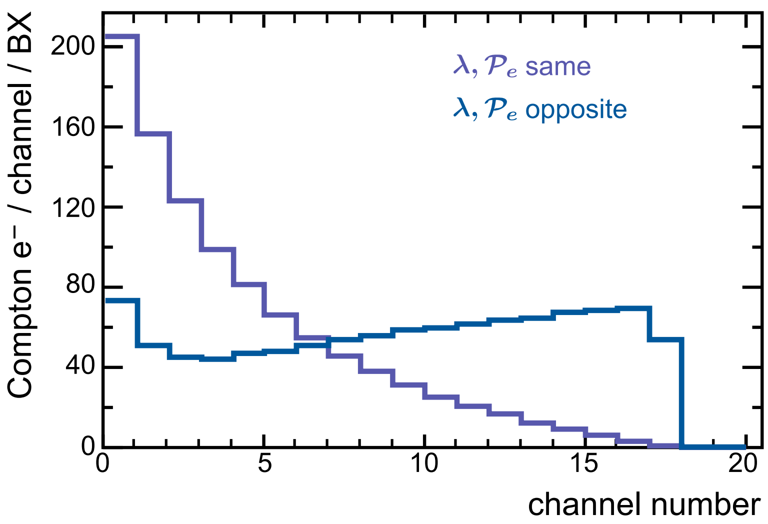

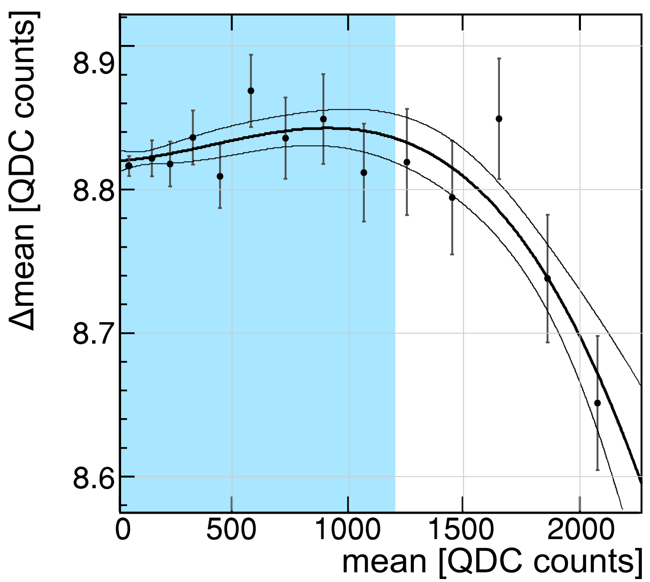

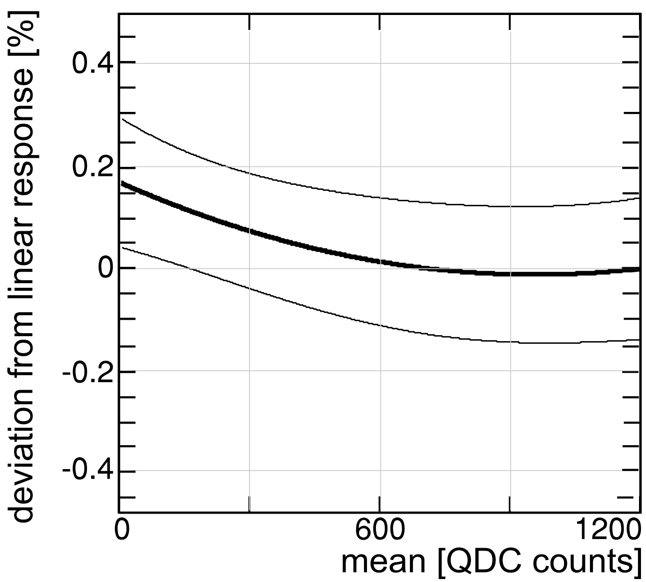

Non-linearity in extreme polarimeter channels.

- up to 210 Compton e^- ($\sim$ 1200 QDC counts)
- overall non-linearity already small in this range (max 0.2 %)
- in single channels even smaller

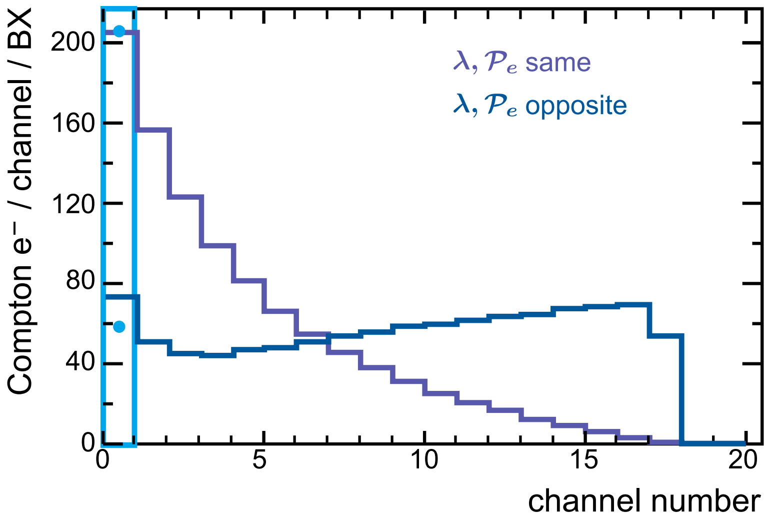

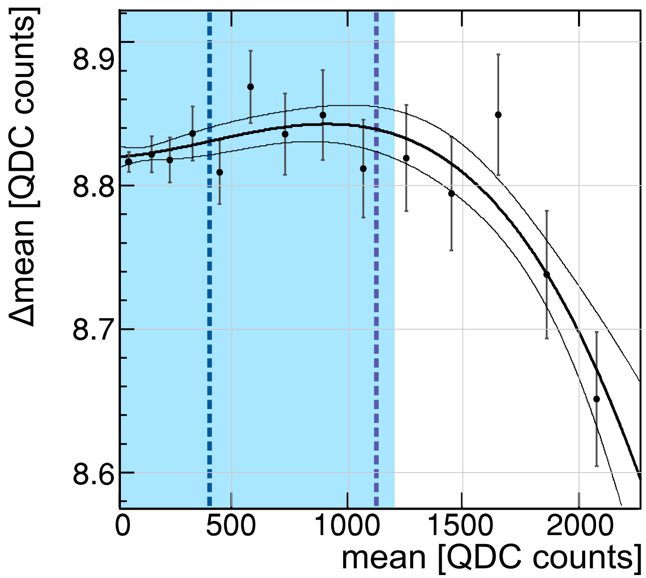

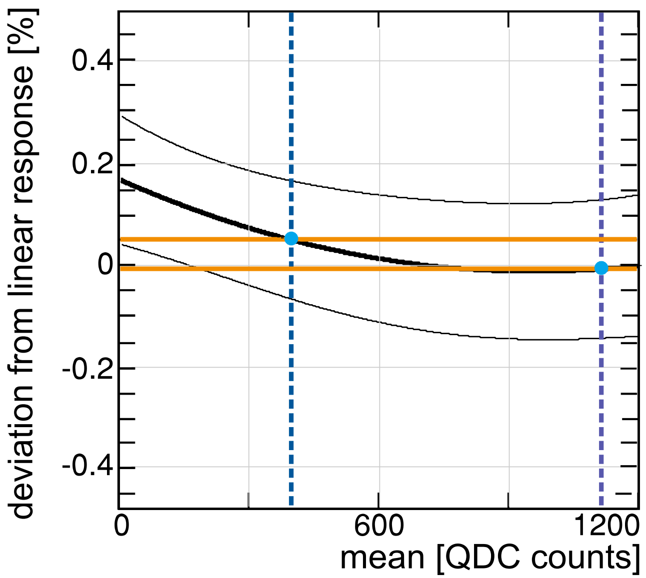

Non-linearity in extreme polarimeter channels.

- up to 210 Compton e^- (∼ 1200 QDC counts)
- overall non-linearity already small in this range (max 0.2 %)
- in single channels even smaller

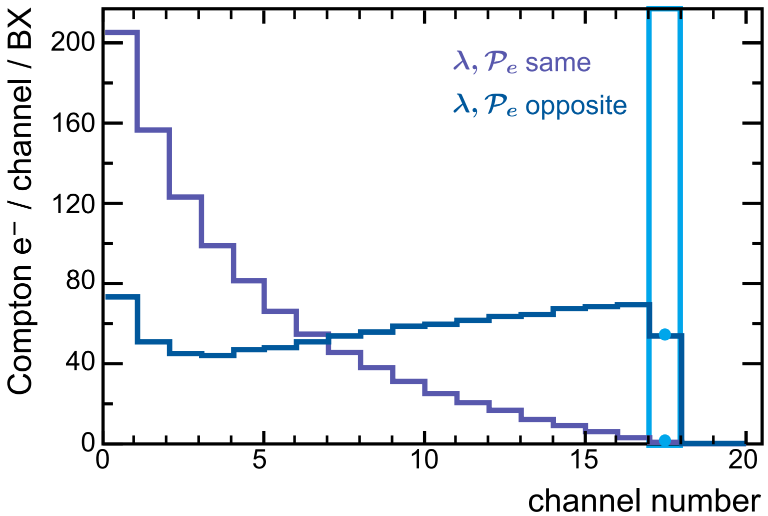

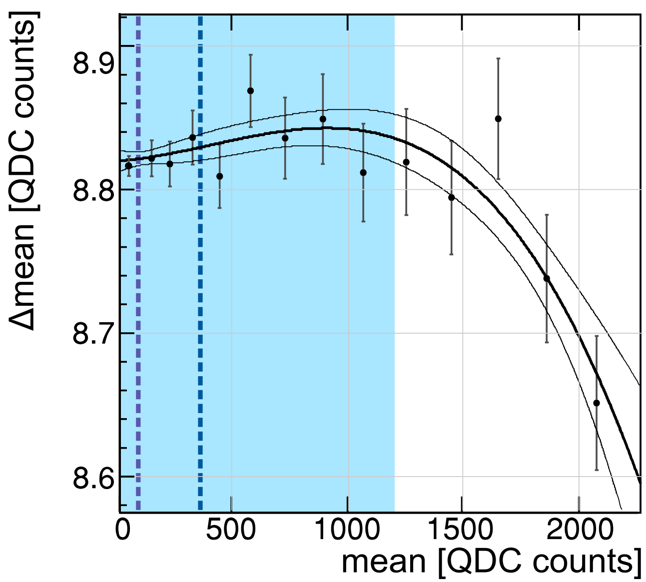

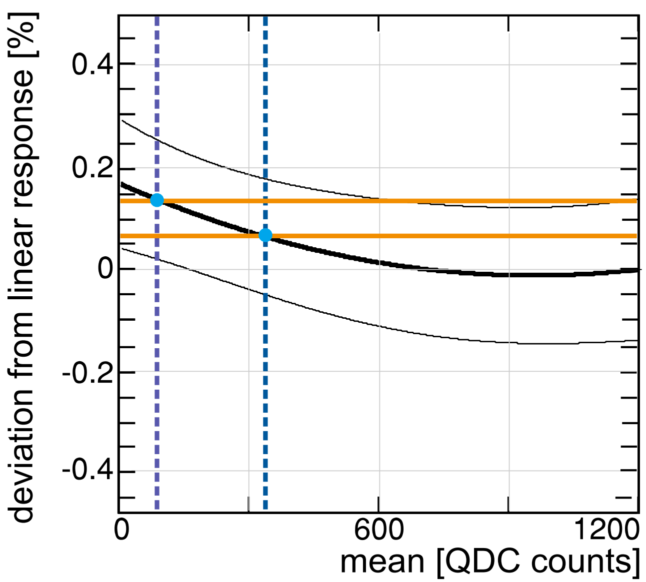

Laser Room.

Downstream Polarimeter

Plan view: Config. of surface laser room, penetration shaft and extraction line tunnel

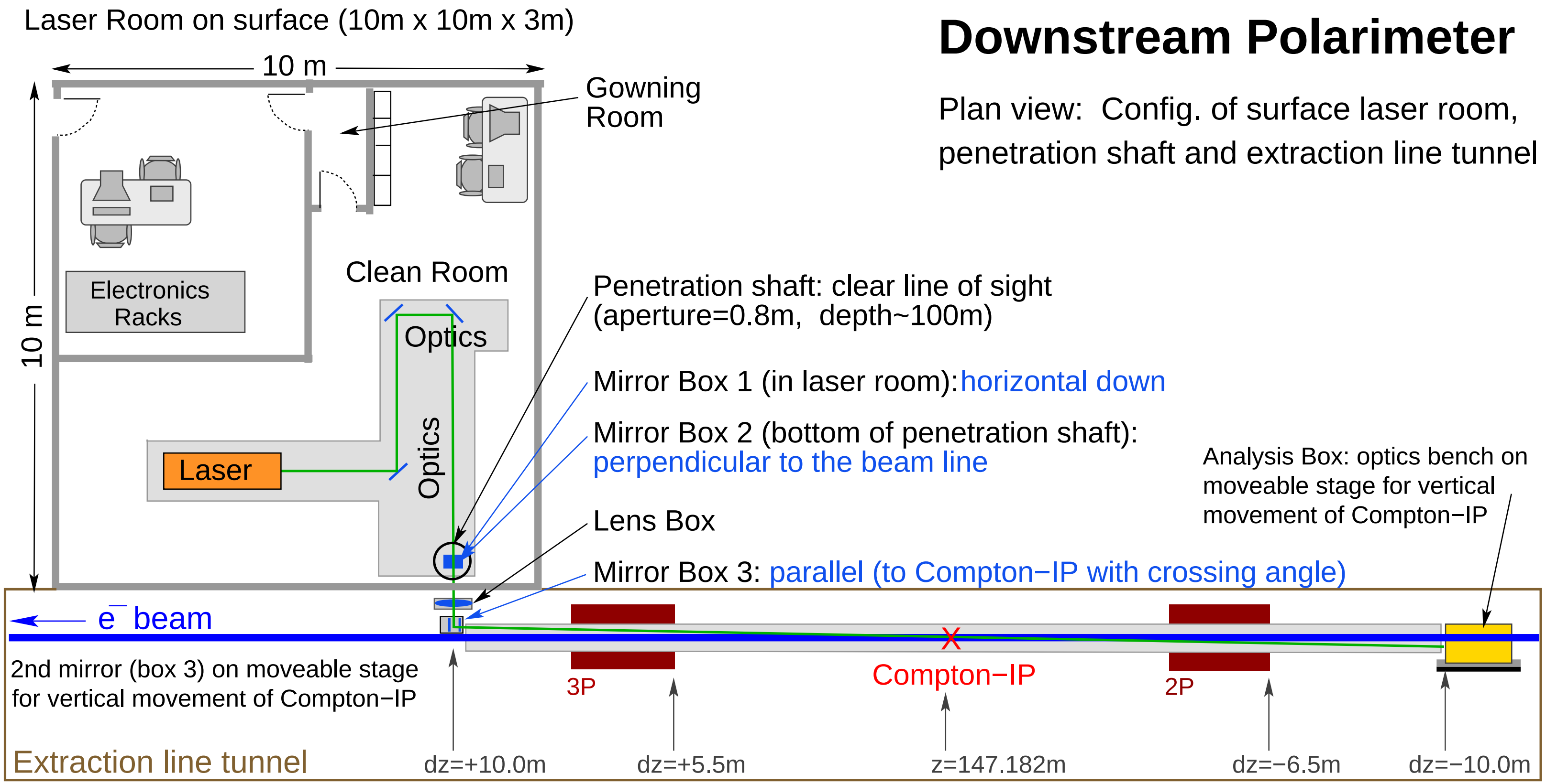

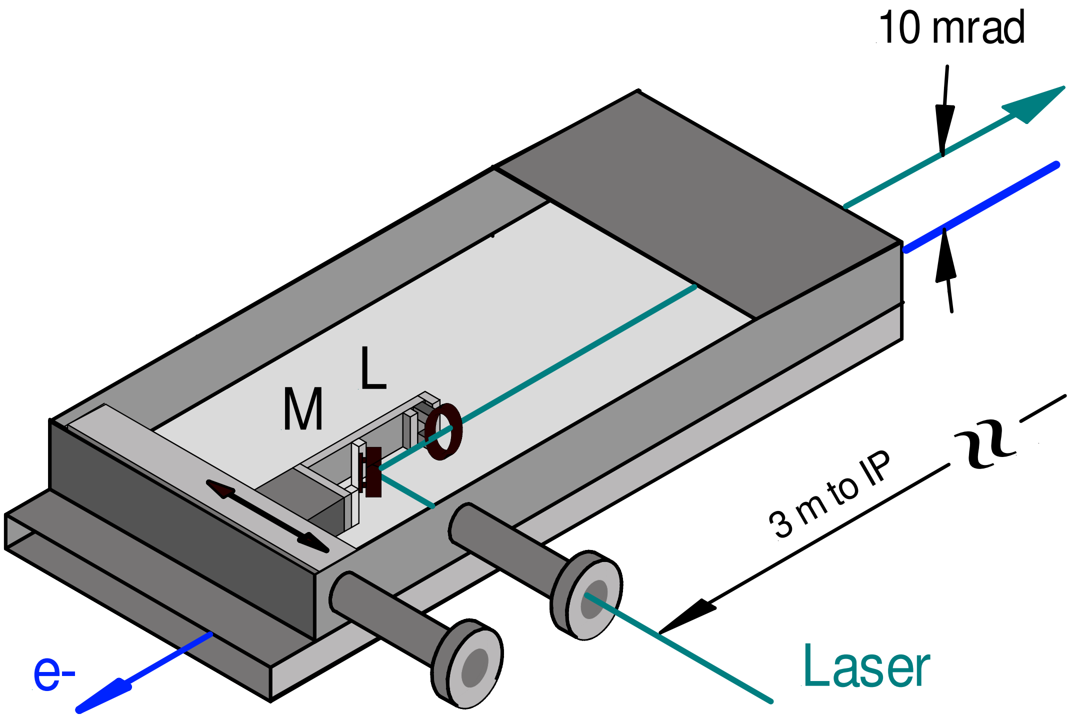

Movable Laser Beam

Spin transport.

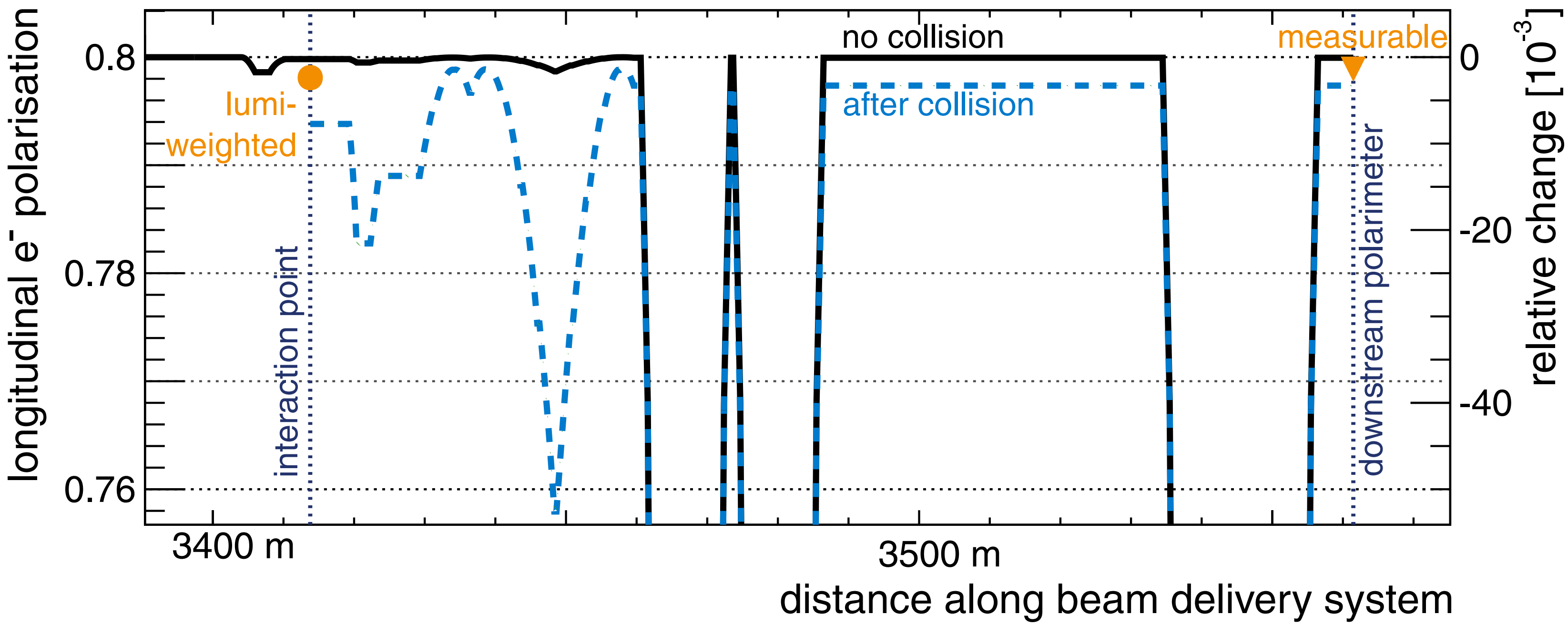

Spin tracking (more).

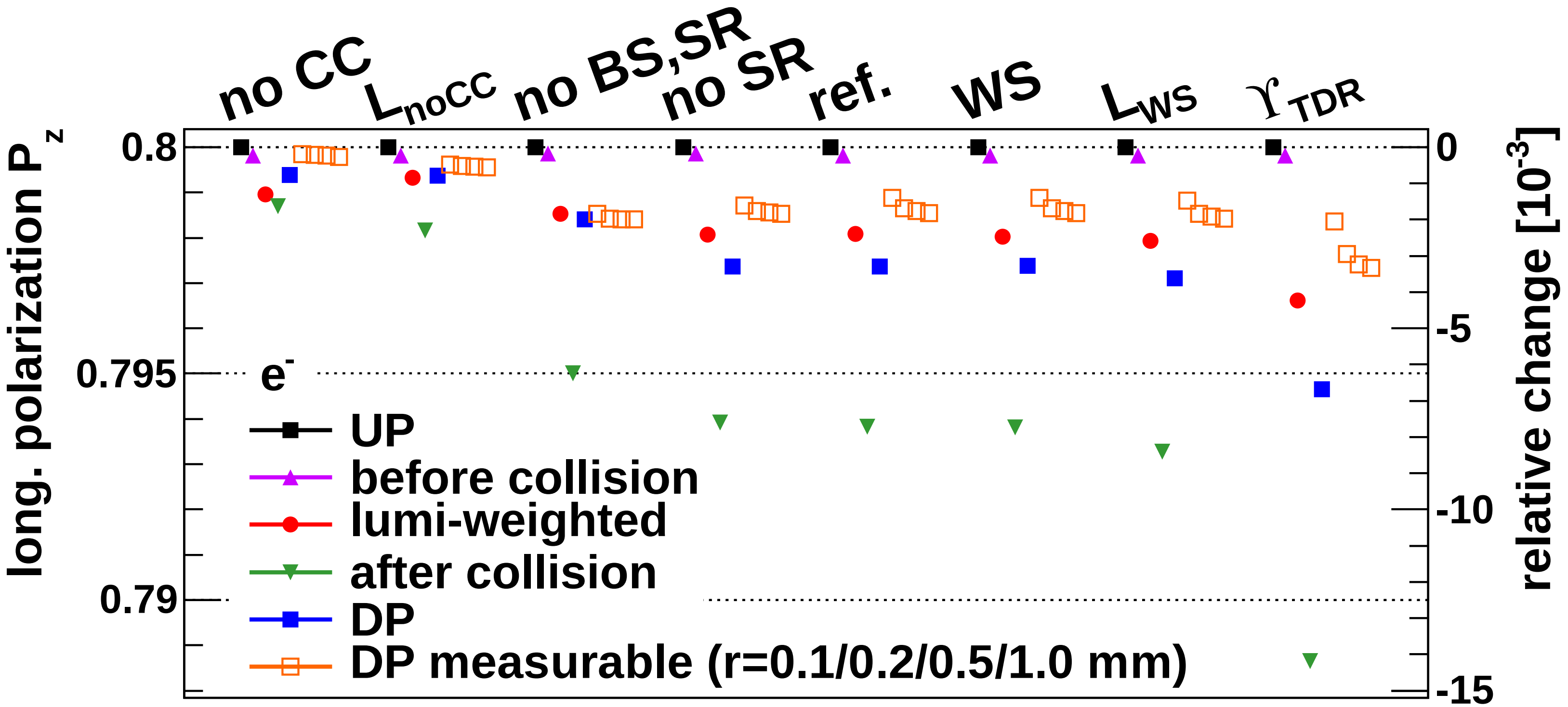

Beam Energy Spectrum After Collision.

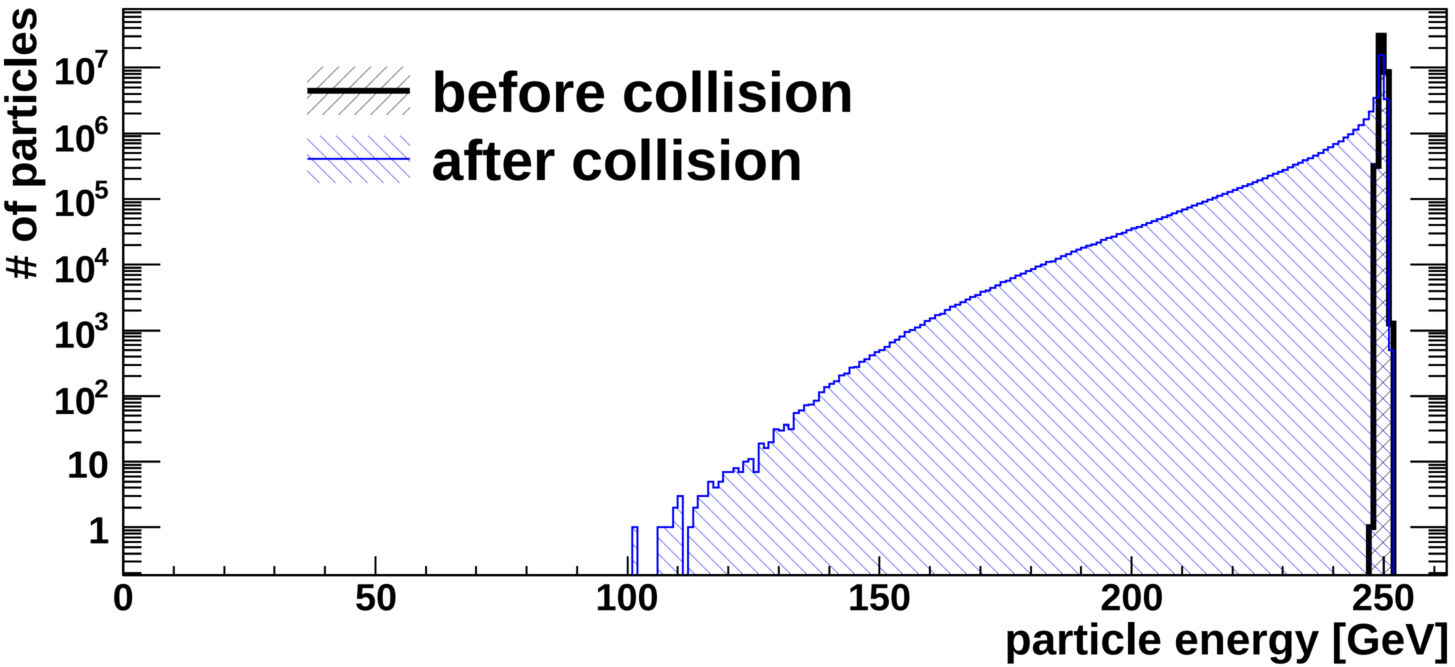

Downstream Polarimeter: y vs E.

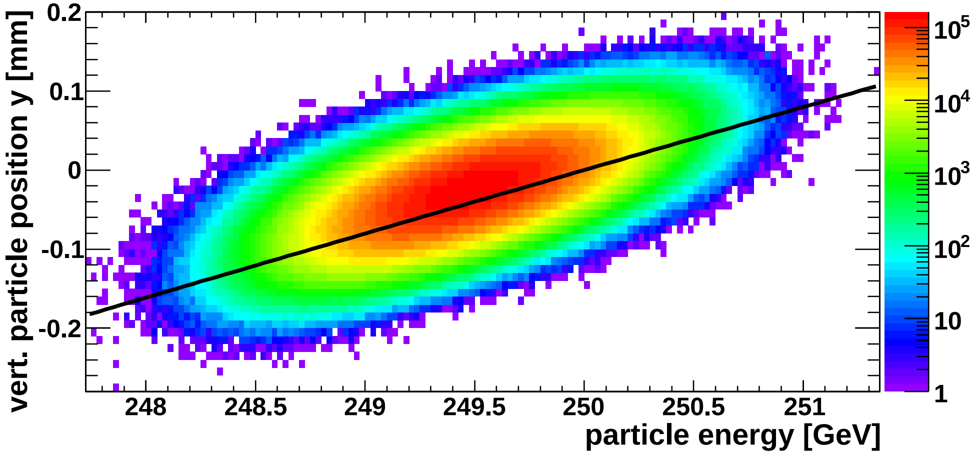

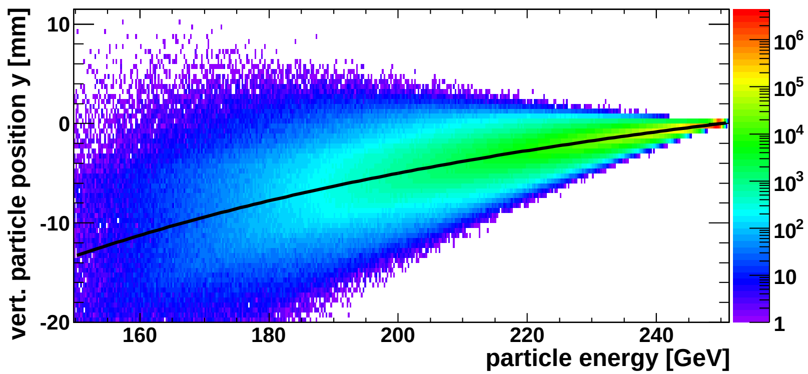

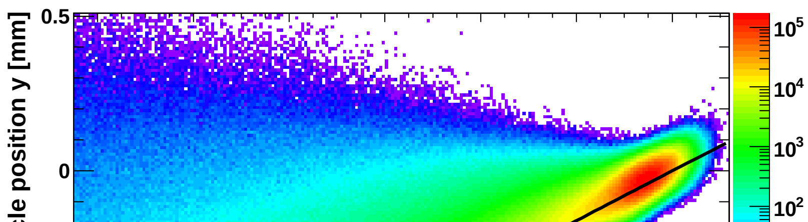

Downstream Polarimeter: P_Z vs E, P_Z vs y.

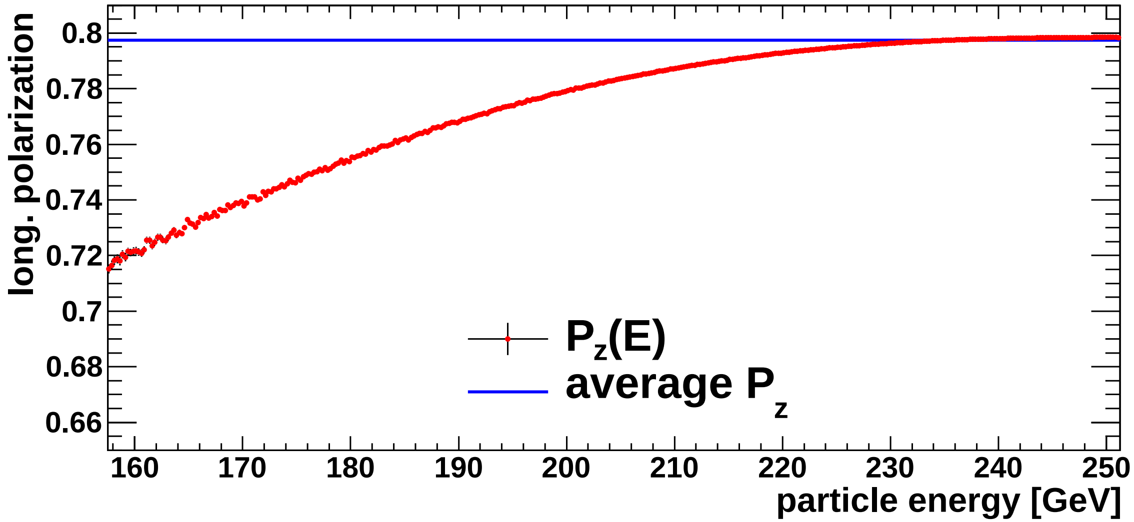

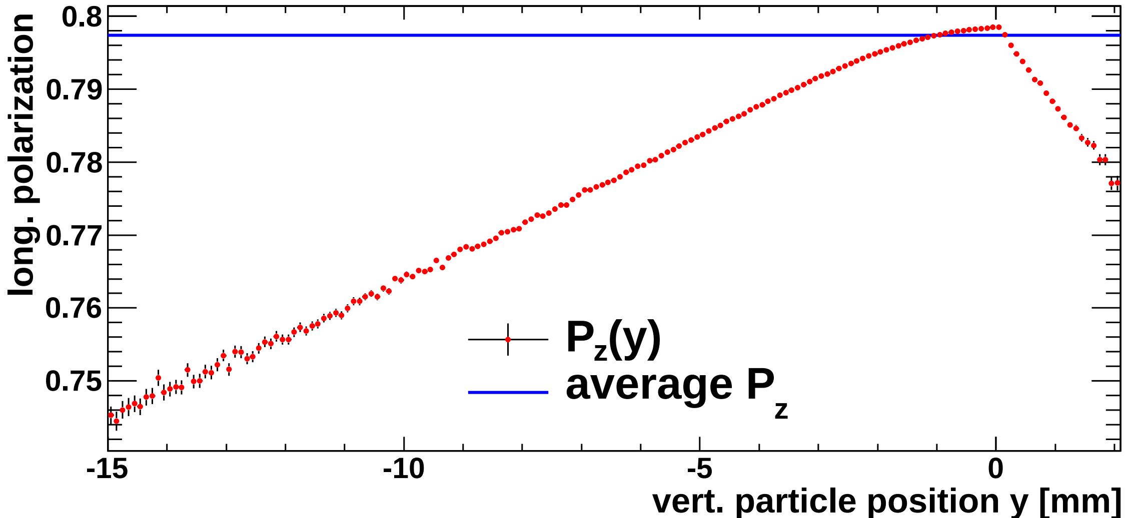

Total Polarisation IP → DP.

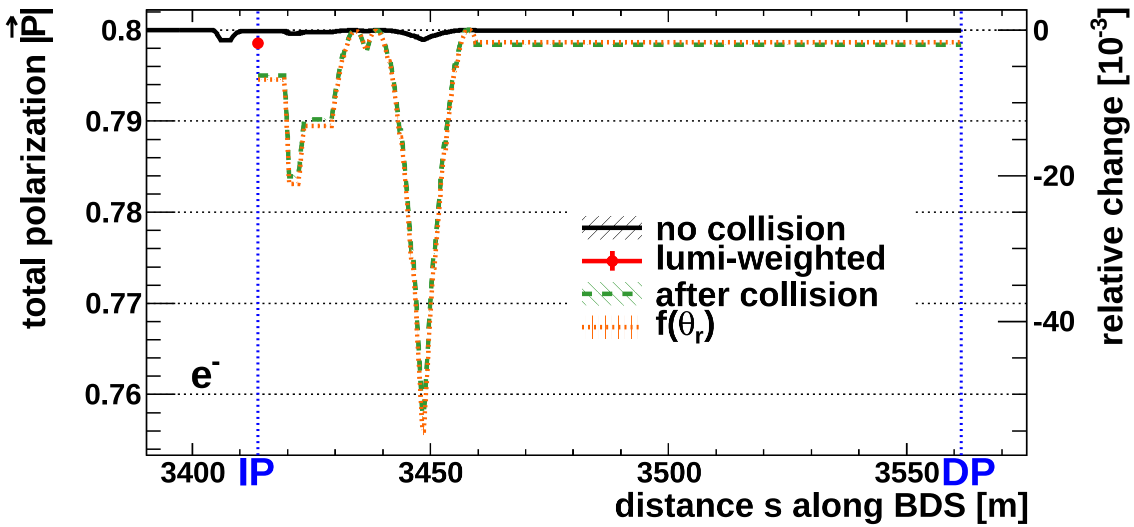

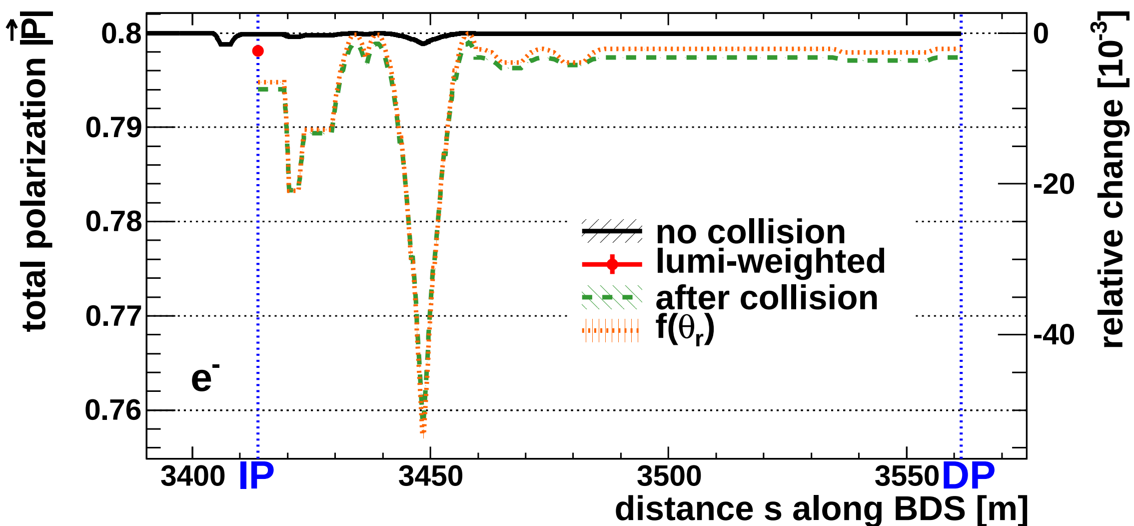

Polarised Cross-sections.

$$\sigma_{P_{e^-} P_{e^+}} = \frac{1}{4} \left\{ (1+P_{e^-})(1+P_{e^+})\sigma_{RR} + (1-P_{e^-})(1-P_{e^+})\sigma_{LL} + (1+P_{e^-})(1-P_{e^+})\sigma_{RL} + (1-P_{e^-})(1+P_{e^+})\sigma_{LR} \right\}$$

processes with s-channel Z/γ exchange only:

- $\sigma_{RR} = \sigma_{LL} = 0$
- $4\sigma_{P_{e^-} P_{e^+}} = (1 - P_{e^-} P_{e^+})(\sigma_{LR} + \sigma_{RL})[1 - P^-_{\mathrm{eff}} A_{LR}]$
- with $P^-_{\mathrm{eff}} = 1 - \frac{P_{e^-} - P_{e^+}}{1 - P_{e^-} P_{e^+}}$ and $A_{LR} = \frac{\sigma_{LR} - \sigma_{RL}}{\sigma_{LR} + \sigma_{RL}}$

general case:

- $\sigma_{RR} \neq \sigma_{LL} \neq 0$
- $4\sigma_{P_{e^-} P_{e^+}} = (1 + P_{e^-} P_{e^+})(\sigma_{LL} + \sigma_{RR})[1 + P^+_{\mathrm{eff}} A_{LLRR}]$ + above
- with $P^+_{\mathrm{eff}} = 1 + \frac{P_{e^-} + P_{e^+}}{1 + P_{e^-} P_{e^+}}$ and $A_{LLRR} = \frac{\sigma_{LL} - \sigma_{RR}}{\sigma_{LL} + \sigma_{RR}}$

Polarisation Averages.

Absolute cross-section measurements require:

- $\langle P_{e^\pm} \rangle_{IP} = \frac{\int P_{e^\pm}(t)\mathcal{L}(t)dt}{\int \mathcal{L}(t)dt}$
- $\langle P_{e^-} P_{e^+} \rangle_{IP} = \frac{\int P_{e^-}(t)P_{e^+}(t)\mathcal{L}(t)dt}{\int \mathcal{L}(t)dt}$
- correlations between lumi and polarisation?!

Direct extraction from collision data

- any abundant, well-known, polarisation dependent process:
- $\langle | P_{e^\pm} | \rangle_{IP} = \sqrt{\frac{(\sigma_{-+}+\sigma_{+-}-\sigma_{--}-\sigma_{++})(\pm\sigma_{-+}\mp\sigma_{+-}+\sigma_{--}-\sigma_{++})}{(\sigma_{-+}+\sigma_{+-}+\sigma_{--}+\sigma_{++})(\pm\sigma_{-+}\mp\sigma_{+-}-\sigma_{--}+\sigma_{++})}}$
- σ_{+-} is total cross-section for $P(e^-, e^+) = (+x\%, -y\%)$, etc.
- assumes $P_+(e^-) = -P_-(e^-)$ and $P_+(e^+) = -P_-(e^+)$

Polarisation Average from Collision Data.

Methods studied sofar

- total cross-sections:
  - *WW* at 500 GeV and 1 TeV (ILD, full sim)
  - single *W* etc at 3 TeV (CLIC, cross-section level)
- single-differential cross-sections:
  - *WW* at 500 GeV and 1 TeV (ILD, full sim)
- double-differential cross-sections:
  - *WW* at 1 TeV (SiD, full sim)

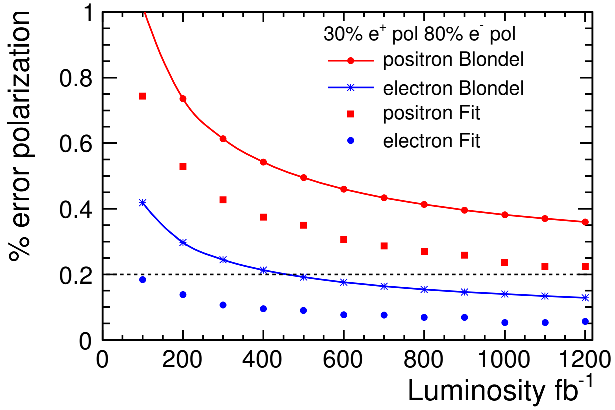

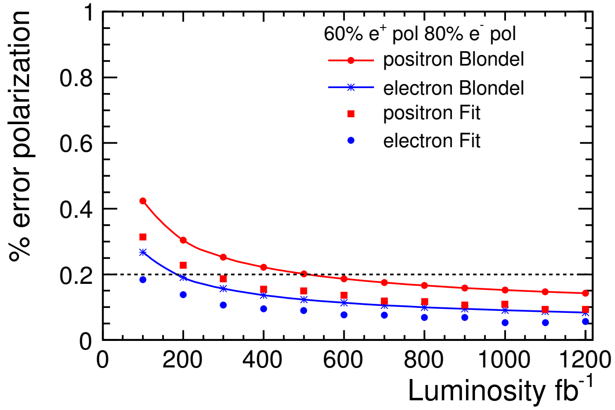

Luminosity Sharing.

How much running time needed for $++$ and $--$?

- like-sign combinations less interesting for SM phyics
- 10% to 20% like-sign lumi rather close to optimum (50%)
- even 2% halfs already total lumi needed for 0.2% precision

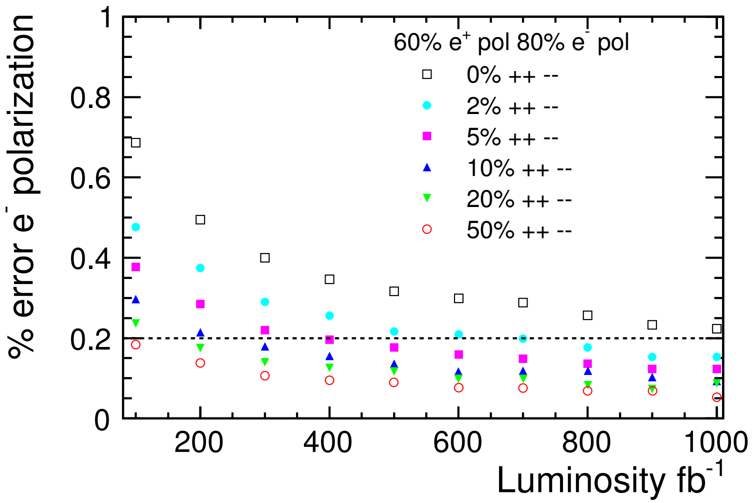

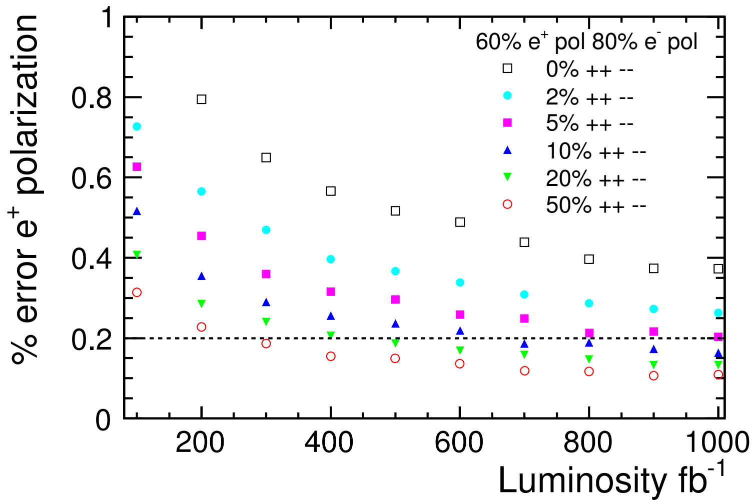

Unequal Polarisations.

What happens if $P_+(e^-) \neq -P_-(e^-)$ and $P_+(e^+) \neq -P_-(e^+)$?

Measure enough cross-sections to determine all polarisations:

- eg single W,Z,γ with $++$, $--$, $+-$, $-+$, $+0$, -0, $0+$, $0-$
- precision significantly worse than for equal $\mid P \mid$ assumption

[cf. G. Wilson, LCWS 2012]

Assume $\mid P \mid$ equal up to $2\epsilon^{\pm}$ – measure $\epsilon^{\pm}$with polarimeters:

- $P_+(e^{\pm}) = P^{\pm} + \epsilon^{\pm}$ and $P_-(e^{\pm}) = P^{\pm} - \epsilon^{\pm}$
- $\delta P_+(e^{\pm})$ (or δA_{LR}) same order of magnitude as $\delta\epsilon^{\pm}$ and $\epsilon^{\pm}$

$\Rightarrow$ need polarimetry at permille-level
and fast helicity reversal for both beams

Impact of Polarimeter Precision.

What happens if $P_+(e^-) \neq -P_-(e^-)$ and $P_+(e^+) \neq -P_-(e^+)$?

- let all P vary independently $\Rightarrow \delta P/P$ in *percent* regime
- better: difference to $\pm\delta P/P|_{pol} = 0.25\%$ with polarimeters
- limits ultimate precision on $P(e^-)$!

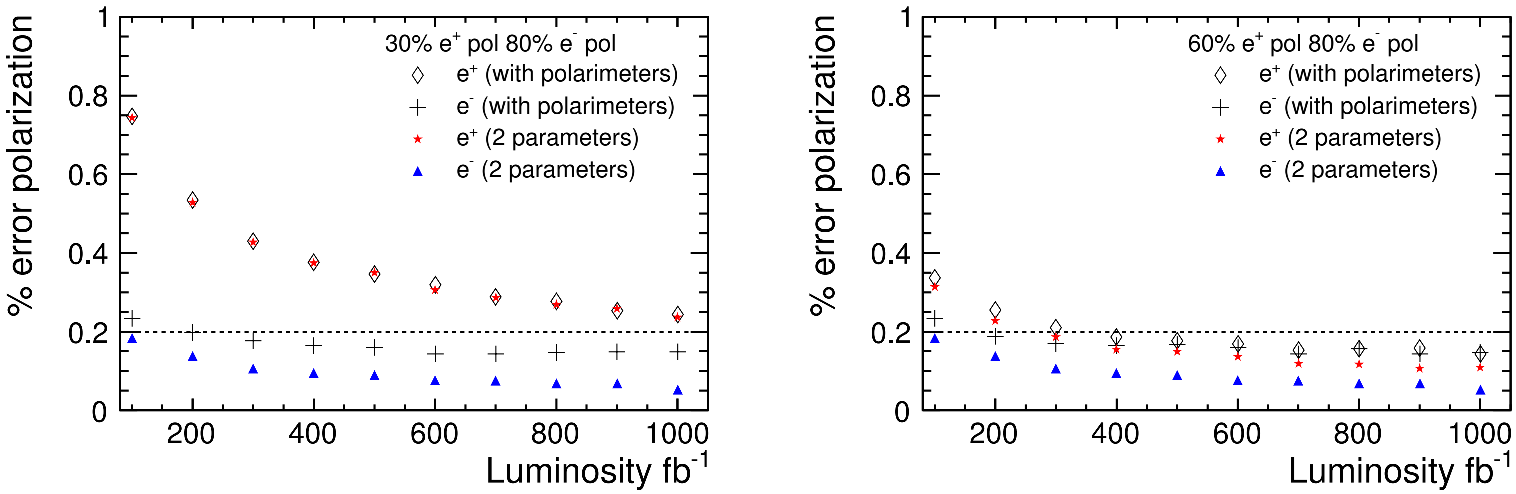

$\Rightarrow$ need polarimetry at permille-level

and fast helicity reversal for both beams

Fast helicity reversal.

... for both beams:

- collect data for all helicity configurations simultaneously
- roughly equal polarisation (absolute) values for all data sets
- cancellation of time dependent effects - also in main detector!

Counter example HERA:

- slow helicity reversal: weeks between flips
- differences in $\langle P_e \rangle_{IP}$: rely on polarimeters
- uncertainty $\sim 2\%$

Collisions	$P_e[\%]$	$\mathcal{L}[\mathrm{pb}^{-1}]$
e^+p	+32	98
e^+p	-38	82
e^-p	+37	46
e^-p	-26	103

Phys. Lett. B704 (2011) 388 [arxiv:1107.3716] (H1 Leptoquarks)

Correction to modified Blondel scheme.

$$P_+(e^\pm) = P^\pm + \epsilon^\pm \text{ and } P_-(e^\pm) = P^\pm - \epsilon^\pm$$